

Neuroprotective mechanism of TMP269, a selective class IIA histone deacetylase inhibitor, after cerebral ischemia/reperfusion injury

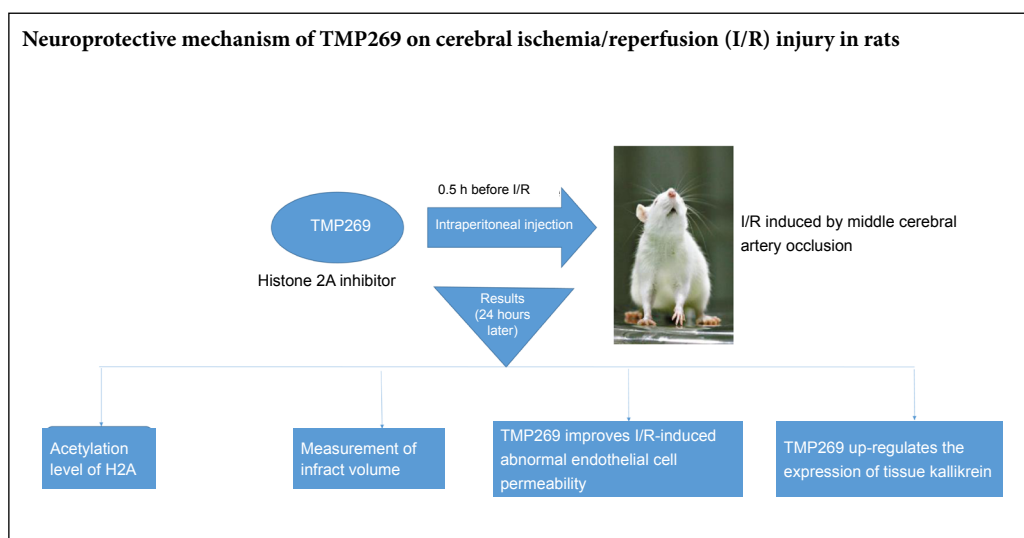
Lu Su^{1,*}, Dan Liang^{2,*}, Shen-Yi Kuang¹, Qiang Dong¹, Xiang Han^{1,*}, Zheng Wang^{1,*}

¹ Department of Neurology, Huashan Hospital, Fudan University, Shanghai, China

² Department of Rehabilitation Medicine, Huashan Hospital, Fudan University, Shanghai, China

Funding: This study was supported by the National Natural Science Foundation of China, No. 81501134 (to ZW).

Graphical Abstract



Abstract

TMP269 is a selective class IIA histone deacetylase inhibitor that has a protective effect on the central nervous system, whose specific mechanism of action is unclear. We aimed to reveal the optimal concentration of TMP269 for protecting against cerebral ischemia/reperfusion injury and its neuroprotective mechanism. Male Sprague-Dawley rats were randomly divided into sham, ischemia/reperfusion, and 1, 4, 10 and 16 mg/kg TMP269 groups. Cerebral ischemia/reperfusion injury was induced by middle cerebral artery occlusion. TMP269 was intraperitoneally administered at different doses 0.5 hours before ischemia induction. Western blot assay and immunohistochemistry were used to detect effects of TMP269 on histone 2 acetylation. The results showed that the level of histone 2 acetylation was increased 24 hours after TMP269 injection. 2,3,5-Triphenyltetrazolium chloride staining was utilized to examine effect of TMP269 on infarct volume. The results found that different doses of TMP269 could reduce the infarct volume. Western blot assay, immunohistochemistry and Evans blue staining were employed to measure the effect of TMP269 on blood-brain barrier. The results showed that TMP269 counteracted the abnormal endothelial cell permeability changes caused by cerebral ischemia/reperfusion. Western blot assay and immunohistochemistry were used to determine the effect of TMP269 on tissue kallikrein. The results found that TMP269 up-regulated the expression of tissue kallikrein. Western blot assay further determined the optimal concentration to be 4 mg/kg. In conclusion, TMP269 plays a neuroprotective role by up-regulating the level of histone 2 acetylation, alleviating endothelial cell injury after cerebral ischemia/reperfusion, and up-regulating the expression of tissue kallikrein. The experimental protocol was approved in 2014 by the Department of Laboratory Animal Science, Fudan University, China (approval No. 20140143C001).

Key Words: blood-brain barrier; drug treatment; endothelial cell permeability; histone deacetylase inhibitor; neuroprotection; stroke; tissue kallikrein; TMP269

Chinese Library Classification No. R453; R364; R741

Introduction

Ischemic stroke is a refractory disease that seriously endangers human life (Mendis et al., 2015; Evans et al., 2017; Wang et al., 2019). Stroke pathogenesis is highly complex and the demand for neuroprotective treatments has not been met (Cheng et al., 2004). The only pharmacological treatment currently approved for ischemic stroke is tissue plasminogen activator in the effective time window, which at 4.5 hours is relatively narrow (Grossman and Broderick, 2013). The treatment of stroke is intensively studied, with epigenetic changes that occur during cerebral ischemia of particular interest. For example, histone deacetylation modification is closely associated with stroke pathophysiology (Lanzillotta et al., 2010, 2013).

Histone deacetylases (HDACs) are divided into four classes according to structure, function and similarity to yeast homologs. They include class I (HDAC1, 2, 3 and 8), class II (HDAC 4, 5, 6, 7, 9 and 10), class III (Sirtuins, SIRT1-7) and class IV (HDAC11). These enzymes can remove acetyl groups from histones and they play a vital role in embryonic development and differentiation of neural cells (Arcidiacono et al., 2018; Večeřa et al., 2018). HDAC inhibitors can block dysregulated activity of HDACs by binding to the active enzymatic sites of class I, II and IV HDACs (Zhang et al., 2018b).

HDAC inhibitors can have a significant effect on many diseases, such as cardiovascular diseases (Rawal et al., 2017; Milan et al., 2018), kidney diseases (Aggarwal et al., 2017; Orillion et al., 2017; Pili et al., 2017), and rheumatic diseases (Oh et al., 2017; Angiolilli et al., 2018). Furthermore, a variety of HDAC inhibitors, used at different times, can protect against ischemic damage or improve long-term functional outcome after stroke (Aune et al., 2015; Kassis et al., 2016). TMP269 is a novel and selective class IIA histone deacetylase inhibitor with IC₅₀s of 126/80/36/9 nM for HDAC 4/5/7/9, respectively (Lobera et al., 2013). We have previously shown that behavioral outcomes, infarct volume, and brain edema in cerebral ischemia/reperfusion injury rats were improved by treatment with TMP269 (Kuang et al., 2018). However, the mechanism of TMP269 action is not fully understood. Our previous investigations were limited to one tight junction protein, occludin, which was not sufficient to confirm the effect of TMP269 on the blood-brain barrier. In addition, we only studied one concentration of TMP269, which did not allow pharmacodynamic studies of the drug. Therefore, here, we examined different concentrations of TMP269 to determine the optimal concentration for neuroprotection. We also studied the effects of TMP269 on three tight junction proteins and explored the effects of TMP269 on the blood-brain barrier using Evans blue staining. Lastly, we investigated changes in tissue kallikrein expression in response to TMP269 to explore the mechanism of TMP269 action.

As we can see, after cerebral ischemia-reperfusion injury, the entire system including tissue kallikrein is activated, leading to a protective effect on nerve damage. Maybe, TMP269 can further enhance its activation after cerebral ischemia-reperfusion injury given its neuroprotective effect.

Materials and Methods

Animals

Adult male Sprague-Dawley rats weighing 250–300 g ($n = 108$) were obtained from Shanghai Jiesijie Animal Corporation, Shanghai, China. The experimental protocol was approved in 2014 by the Department of Laboratory Animal Science, Fudan University, China (approval No. 20140143C001).

Animal model of ischemia/reperfusion (I/R)

Ischemia was induced by left middle cerebral artery occlusion. Anesthesia was intraperitoneally induced with 10% chloral hydrate (350 mg/kg) and the body temperature was kept at 37°C with an electric blanket. A nylon thread with a silicone tip (Beijing Cinontech Co., Ltd., Beijing, China) was advanced from the external carotid artery into the internal carotid artery. Ninety minutes later, the nylon thread was withdrawn to allow reperfusion. After surgery, rats were individually housed and given access to food and water. Once animals recovered from anesthesia, they were scored based on Bederson's scale (Bederson et al., 1986). Rats with a score below 2 were excluded. Bederson's scale is divided into four functional grades: 0, no symptoms of neurological damage; 1, in the tail suspension test the contralateral forepaw does not fully extend indicating mild forelimb weakness; 2, the forelimb does not resist contralateral push indicating severe forelimb weakness; 3, compulsory circling behavior.

After reperfusion for 24 hours, rats were anesthetized again and euthanized for further experiments. The sham group was treated the same as the experimental group except that the nylon thread was not inserted into the internal carotid artery.

Group allocation and TMP269 administration

Rats were randomly divided into sham ($n = 24$), I/R (cerebral I/R, $n = 24$), 1 mg/kg TMP269 (cerebral I/R combined with 1 mg/kg TMP269, $n = 12$), 4 mg/kg TMP269 (cerebral I/R combined with 4 mg/kg TMP269, $n = 24$), 10 mg/kg TMP269 (cerebral I/R combined with 10 mg/kg TMP269, $n = 12$), and 16 mg/kg TMP269 (cerebral I/R combined with 16 mg/kg TMP269, $n = 12$) groups. TMP269 (Selleck, Houston, TX, USA) was intraperitoneally administered half an hour before induction of ischemia.

Western blot assays

Ipsilateral cortical tissue surrounding the ischemic zone was harvested from euthanized animals. Cortical protein was extracted and western blot assays were performed as previously described (Yi et al., 2004). Proteins were separated by 10% or 12% sodium dodecyl sulfate-polyacrylamide gel electrophoresis and transferred to polyvinylidene fluoride membranes. After blocking for 1 hour, the membranes were incubated overnight with primary antibodies in primary antibody dilution buffer (Beyotime) at 4°C overnight. The following primary antibodies were used: rabbit polyclonal anti-histone 2 acetylation (H2A) (acetyl) (Cat#177308; 1:1000; Abcam, Cambridge, MA, USA), rabbit monoclonal anti- β -actin

(Cat#179467; 1:1000; Abcam), rabbit polyclonal anti-occludin (Cat#710192; 1:1000; Thermo Fisher, Waltham, MA, USA), rabbit polyclonal anti-claudin-5 (Cat#34-1600; 1:1000; Thermo Fisher), rabbit polyclonal anti-ZO-1 (Cat#61-7300; 1:1000; Thermo Fisher), rabbit polyclonal anti-tissue kallikrein (Cat#131029; 1:1000; Abcam). Membranes were then washed and incubated with a goat anti-rabbit IgG secondary antibody (1:2000; Sigma, St. Louis, MO, USA), at room temperature for 1 hour. An electro-chemi-luminescence kit was used to treat the membranes and develop the signal. Finally, Bio-Rad imaging system (Bio-Rad, CA, USA) was used for detection. Gray values were analyzed by ImageJ software (Bethesda, MD, USA).

Immunohistochemistry

After anesthesia, rats were perfused through the heart with 4% paraformaldehyde and the brains were then dissected. Paraffin sections were prepared and then dewaxed and hydrated. Sections were washed three times with phosphate buffered saline (PBS), incubated with 3% hydrogen peroxide at room temperature for 10 minutes, and then rinsed three times with PBS. After heat-induced antigen retrieval, sections were treated with normal bovine serum in PBS for 30 minutes at room temperature. Primary antibodies were then added and incubated at 4°C for 18 hours. After rinsing three times with PBS, the secondary antibody was added and incubation continued for 20 minutes. Sections were then washed three times with PBS. Staining was visualized using DAB and the sections were then observed. Finally, sections were further dyed and sealed with hematoxylin. Antibodies used were rabbit polyclonal anti-H2A acetyl (Cat#45152; 1:500; Abcam), rabbit polyclonal IgG anti-tissue kallikrein (1:500; Cat#131029; Abcam), goat anti-rabbit antibody (1:200; Sigma) and rabbit anti-rat antibody (1:500; Sigma). To display the results more intuitively, the average optical density of positive areas (40×) was calculated using Imagepro Plus 6 software (Media Cybernetics, Silver Spring, MD, USA).

Evans blue staining

One hour before rats were euthanized, 2% Evans blue physiological saline (4 mL/kg) was injected into the femoral vein. After opening the chest and infusing, the brain was dissected and 20 μm thick frozen sections were prepared on glass slides. The slides were dried in the dark and sealed with PBS-buffered glycerin. Leakage of Evans blue in brain tissue was observed using a fluorescence microscope (Olympus, Center Valley, PA, USA) with green light excitation.

Lesion analysis

Twenty-four hours after I/R, cerebral infarction volumes were measured by 2,3,5-triphenyltetrazolium chloride (TTC) staining. Brains were dissected and stained with TTC. Starting 3 mm from the frontal pole, continuous 2 mm thick coronal slices were cut from front to back. Brain slices were soaked in 2% TTC phosphate buffer at 37°C for 15 minutes away from light. Normal brain tissue was stained rose red and infarct areas were white. After staining, sections were

photographed and infarct size was calculated (Ding et al., 2006). The red and white areas were measured using a multimedia image analysis system, and the infarct volume percentage was calculated by the following formula: Infarction ratio = $(V_c - V_l)/(V_c \times 2) \times 100\%$; V_c = diameter $\times \Sigma A_c$ (A_c : contralateral volume); V_l = diameter $\times \Sigma A_l$ (A_l : ipsilateral volume) (Numagami and Ohnishi, 2001; Bora and Sharma, 2011).

Statistical analysis

Statistical analyses were performed using SPSS 17.0 statistical software (SPSS, Chicago, IL, USA). Group differences were analyzed using a one-way analysis of variance followed by Duncan's (Duncan's new multiple range) *post hoc* test. Statistical significance of physiological variables was determined with an independent sample *t*-test. *P* values < 0.05 were considered statistically significant.

Results

Level of histone H2A acetylation in the motor cortex increases after TMP269 injection

Histone H2A acetylation was measured by western blot assays. TMP269 up-regulated H2A acetylation compared with the I/R group ($P < 0.001$), and the optimal concentration was 4 mg/kg (Figure 1A). In addition, immunohistochemistry showed that the number of positive cells in the infarct area was increased and the nucleus was more deeply stained in the 4 mg/kg TMP269 group compared with the I/R group (Figure 1B). Quantitative analysis confirmed that acetyl-H2A was significantly upregulated in the 4 mg/kg TMP269 group compared with the I/R group ($P < 0.001$; Figure 1B).

Different concentrations of TMP269 ameliorate cerebral injury after ischemic stroke to varying degrees

Ischemia in the left hemisphere was induced by middle cerebral artery occlusion and infarct size was determined at 24 hours after reperfusion. TTC assay results demonstrated that infarct volume was reduced by TMP269 compared with the I/R group ($P < 0.001$) and that 4 mg/kg TMP269 produced the biggest reduction in infarct size (Figure 2).

TMP269 counteracts abnormal endothelial cell permeability

TMP269 increased expression of the tight-junction proteins, ZO-1, Occludin and Claudin-5 compared with the I/R group ($P < 0.01$; Figure 3A). Blood-brain barrier integrity was assessed by observing the extravasation of Evans blue which is found in the brain when the blood-brain barrier is not intact (Figure 3B). Under green excitation, Evans blue produces bright red fluorescence. Almost no red fluorescence was observed in the sham group. The I/R group had the highest fluorescence intensity, and TMP269 groups showed decreased fluorescence intensity compared with the I/R group.

Immunohistochemistry showed positive neurofilament staining after I/R, which was still present but weaker in the TMP269 group (Figure 3C) compared with the I/R group ($P < 0.001$).

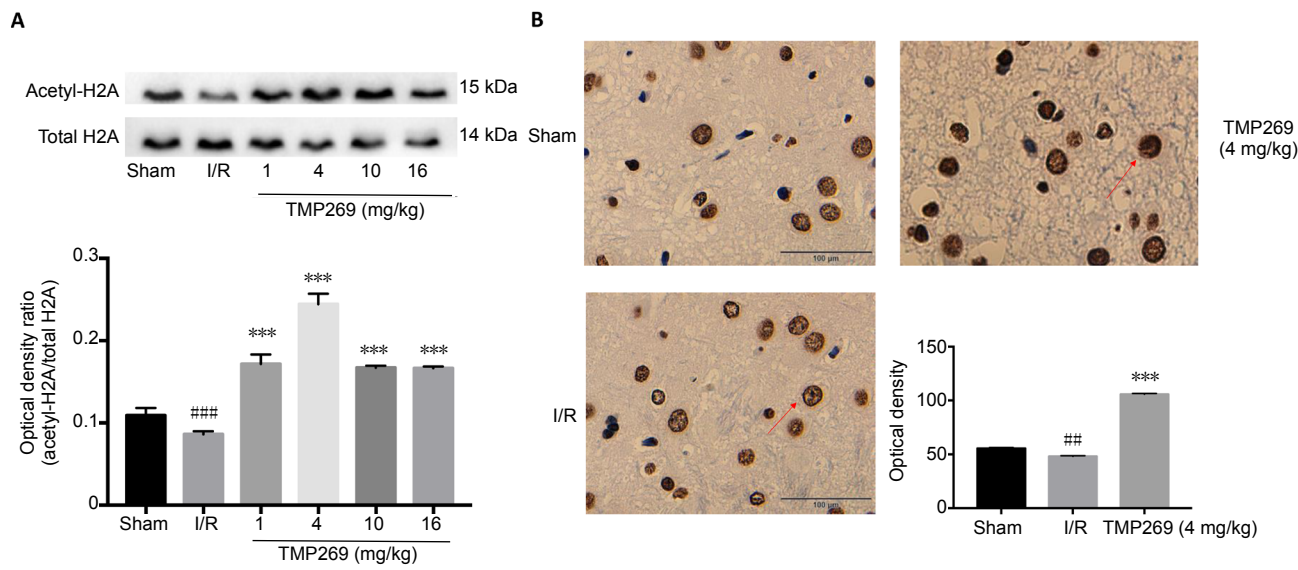


Figure 1 Acetylation of histone H2A increases in the motor cortex of rats after TMP269 treatment. (A) Western blot assay of histone H2A acetylation in the ischemic cerebral hemisphere of rats under different concentrations of TMP269 after reperfusion. (B) Immunohistochemistry images and quantitative analysis of mean optical densities show that the number of positive cells in the infarct area was increased and the nucleus was deeply stained in the TMP269 group. The red arrows indicate the nucleus; histone H2A is expressed in nucleus; and the deeper the staining, the more expression of acetylation of histone H2A. Data are expressed as the mean ± SD ($n = 6$; one-way analysis of variance followed by Duncan's *post hoc* test). $***P < 0.001$, vs. I/R group; $##P < 0.01$, $###P < 0.001$, vs. sham group. Scale bars: 100 μm . I/R: Ischemia/reperfusion.

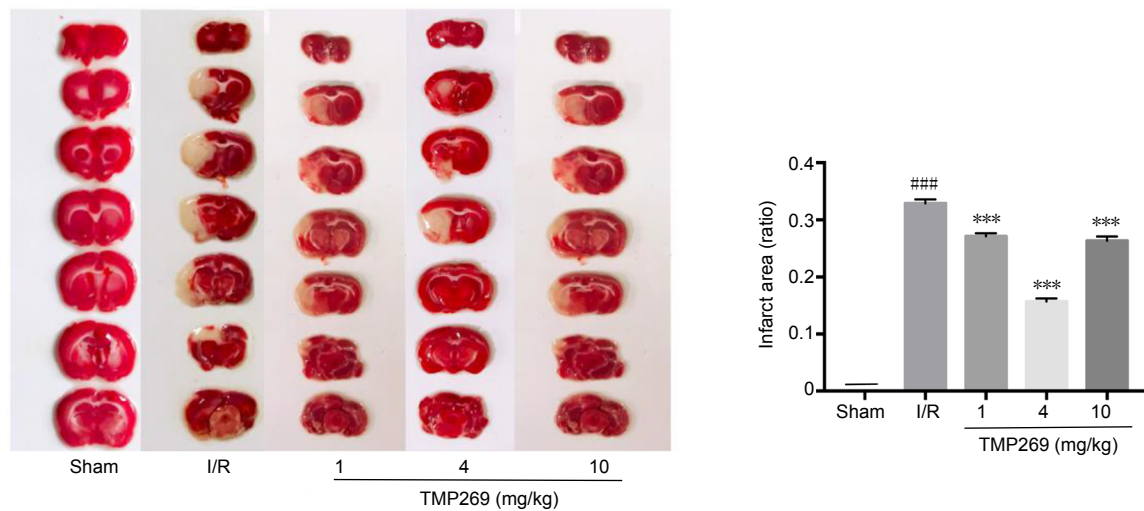


Figure 2 Measurement of infarct volume. The white zone represents damaged brain areas resulting from ischemia. The red zone represents normal brain tissue. Infarct volume was calculated in ischemic rats after 1.5 hours of middle cerebral artery occlusion and 24 hours of reperfusion (I/R). Data are expressed as the mean ± SD ($n = 6$; one-way analysis of variance followed by Duncan's *post hoc* test). $***P < 0.001$, vs. I/R group; $###P < 0.001$, vs. sham group. I/R: Ischemia/reperfusion.

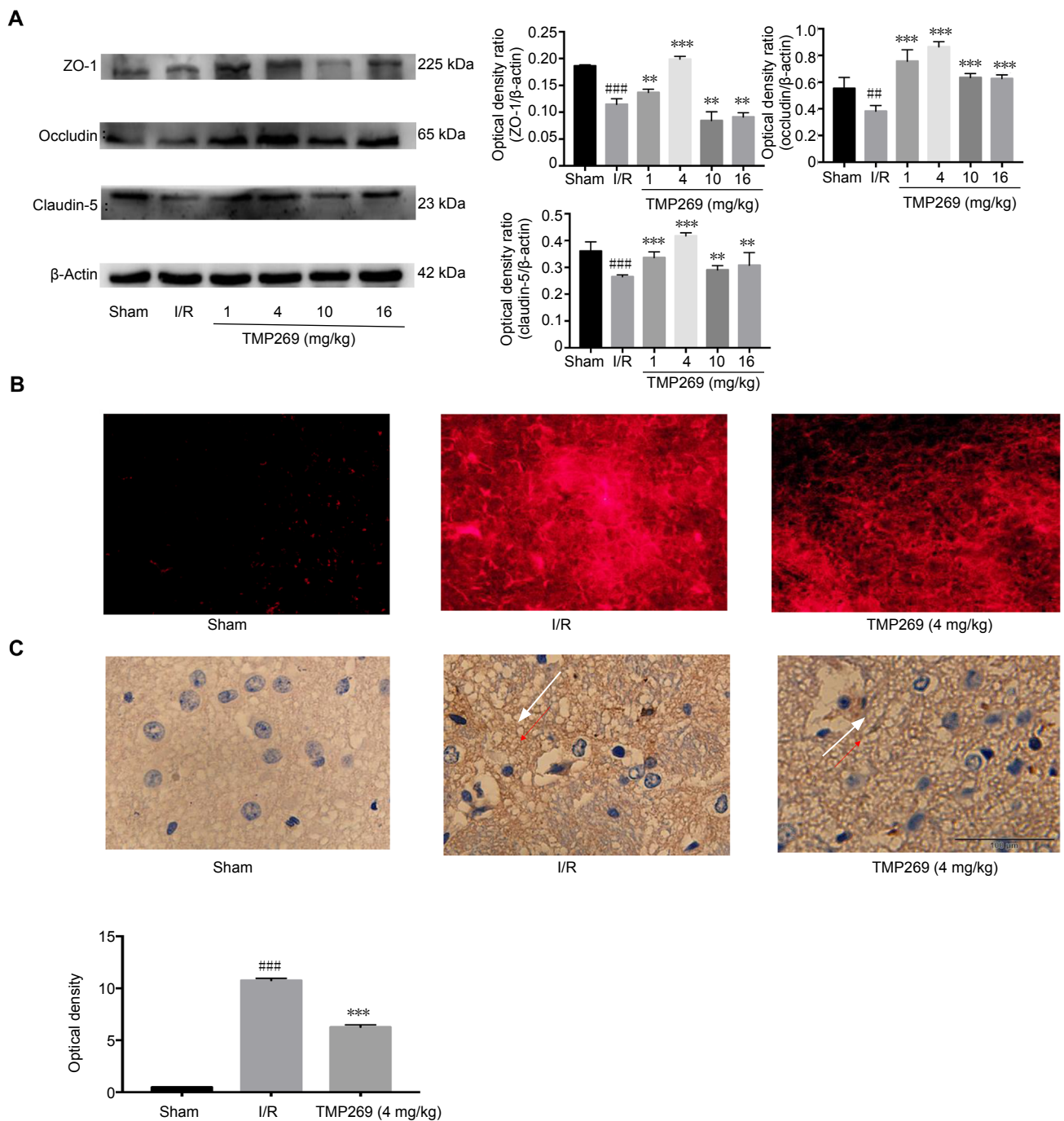


Figure 3 TMP269 improves I/R-induced abnormal endothelial cell permeability.

(A) Representative western blots and quantified data showing tight-junction protein levels in ischemic rats after 1.5 hours of middle cerebral artery occlusion and 24 hours of reperfusion (I/R). (B) Immunofluorescence images of brain sections after injection of Evans blue compared with the sham group. (C) Immunohistochemistry images and quantitative analysis of mean optical density showing neurofilament staining in different groups. The white arrows indicate the nerve fiber network; IgG leaked into the nerve fiber network of the extravascular space after brain injury. The darker the coloration, the more severe the damage. Scale bar: 100 μ m. Data are expressed as the mean \pm SD ($n = 6$). ** $P < 0.01$, *** $P < 0.001$, vs. I/R group; ## $P < 0.01$, ### $P < 0.001$, vs. sham group. I/R: Ischemia/reperfusion.

TMP269 regulates tissue kallikrein expression

Tissue kallikrein expression was increased in the TMP269 groups compared with the I/R group ($P < 0.01$; **Figure 4A**). In addition, immunohistochemistry showed an increased number of positive cells in the infarct area and deeply stained plasma in the 4 mg/kg TMP269 group (**Figure 4B**). Quantitative analysis demonstrated significant upregulation of tissue kallikrein in the 4 mg/kg TMP269 group compared with the I/R group ($P < 0.001$; **Figure 4B**).

Discussion

The pathophysiological mechanism of ischemic stroke is characterized by neuronal death, inflammation, blood-brain barrier destruction and other tissue damage (Rana et al., 2018; Zhang et al., 2018a). Currently, there is no effective therapeutic drug (Smith, 2004). A large number of studies have shown that protein acetylation levels are decreased in the brain after ischemic stroke and HDAC inhibitors are of increasing interest in stroke research.

Class IIA HDACs play an important role in brain development (Sugo et al., 2010; Sando III et al., 2012). TMP269, a selective class IIA HDAC inhibitor, can improve behavioral outcomes and reduce infarct size in cerebral ischemia/reperfusion injury rats. However, the specific mechanism for this action has not been verified. The effective concentration curve of TMP269 has not been determined and it is not known whether TMP269 truly improves endothelial cell abnormalities.

In this study, we examined acetylation changes of histone H2A in the cerebral cortex before and after inhibitor treatment and found that TMP269 can up-regulate the expression of H2A acetylation, especially at a concentration of 4 mg/kg. In addition, TTC staining indicated that the protective effect was most significant at 4 mg/kg. The possible reasons for this being the most effective dose are that TMP269 is dissolved in dimethyl sulfoxide and its toxicity increases as the injection dose increases. Alternatively the metabolism of TMP269 may be relevant; however, further investigation into TMP269 pharmacokinetics is needed to clarify this possibility.

Dysfunction of the vascular endothelium plays an important role in the pathogenesis of many human diseases, such as stroke, cardiovascular disease and chronic kidney failure (Rajendran et al., 2013). In particular, brain endothelial cells are the structural basis of the blood-brain barrier, which can restrict the entry of molecules and immune cells from the systemic circulation into the central nervous system (Siererra et al., 2011). Tight junctions between endothelial cells are essential for maintaining blood-brain barrier integrity. The tight junction complex is composed of transmembrane proteins, cytoplasmic attachment proteins, and cytoskeletal proteins. Transmembrane proteins include three complete membrane proteins, Occludin, Claudin-5, and junctional adhesive molecule. Previously, we only studied the effect of TMP269 on occludin. In this study, we also studied claudin-5 and ZO-1 and performed Evans blue staining. Our results confirm that TMP269 improves the abnormal permeability of endothelial cells.

An important component of the kallikrein-kinin system is tissue kallikrein, a serine proteinase capable of cleaving kininogen to produce the nonapeptide bradykinin, which binds to the constitutively expressed bradykinin 1 and 2 receptors. Exogenous tissue kallikrein can protect against hypoglycemia-induced glutamate excitotoxicity and neurotoxicity caused by acidosis through extracellular signal-regulated kinases 1/2 in primary cultured neurons (Liu et al., 2009, 2011; Su et al., 2011). In addition, exogenous tissue kallikrein has achieved a positive clinical effect by intravenous administration in the acute phase. However, the regulation of endogenous tissue kallikrein is poorly understood. In this experiment, TMP269 up-regulated the expression of endogenous tissue kallikrein in the motor cortex. This provides a rationale for novel treatment strategies combining TMP269 with endogenous tissue kallikrein. Further investigation of TMP269 pharmacokinetics is needed and in future we will explore the effects of TMP269 on rats at different time points.

In conclusion, TMP269 counteracted endothelial cell injury and histone H2A is a critical protein that links ischemic cerebral injury to upregulated tissue kallikrein in experimental stroke. TMP269 has mainly been investigated on a cell biology basis (Sinnott-Smith et al., 2014; Kikuchi et al., 2015) and few animal experiments and no clinical trials have been reported concerning TMP269 in I/R injury. Taken together, our experiments provide evidence for the clinical potential of TMP269 and the relationship between endogenous tissue kallikrein and TMP269 may provide a new target for stroke treatment. In the future, improved understanding of the mechanism of TMP269 action may also indicate new strategies for the treatment of stroke.

Author contributions: Study design: ZW; study guidance: XH; experimental implementation: LS, DL, QD and SYK; data analysis, paper writing: LS. All authors approved the final version of the paper.

Conflicts of interest: The authors declare that there are no conflicts of interest associated with this manuscript.

Financial support: This study was supported by the National Natural Science Foundation of China, No. 81501134 (to ZW). The funding sources had no role in study conception and design, data analysis or interpretation, paper writing or deciding to submit this paper for publication.

Institutional review board statement: The experiment was approved by the Department of Laboratory Animal Science, Fudan University, China (approval No. 20140143C001) in 2014. The experimental procedure followed the United States National Institutes of Health Guide for the Care and Use of Laboratory Animals (NIH Publication No 85-23, revised 1996).

Copyright license agreement: The Copyright License Agreement has been signed by all authors before publication.

Data sharing statement: Datasets analyzed during the current study are available from the corresponding author on reasonable request.

Plagiarism check: Checked twice by iThenticate.

Peer review: Externally peer reviewed.

Open access statement: This is an open access journal, and articles are distributed under the terms of the Creative Commons Attribution-Non-Commercial-ShareAlike 4.0 License, which allows others to remix, tweak, and build upon the work non-commercially, as long as appropriate credit is given and the new creations are licensed under the identical terms.

Open peer reviewer: Sidharth Mehan, Rajendra Institute of Technology & Sciences, India; Min Ye, Nanjing Benq Hospital, China.

Additional file: Open peer review reports 1 and 2.

References

- Aggarwal R, Thomas S, Pawlowska N, Bartelink I, Grabowsky J, Jahan T, Cripps A, Harb A, Leng J, Reinert A (2017) Inhibiting histone deacetylase as a means to reverse resistance to angiogenesis inhibitors: phase I study of abexinostat plus pazopanib in advanced solid tumor malignancies. *J Clin Res Oncol* 35:1231-1239.
- Angiolilli C, Kabala PA, Grabiec AM, Rossato M, Lai WS, Fossati G, Mascagni P, Steinkühler C, Blackshear PJ, Reedquist KA (2018) Control of cytokine mRNA degradation by the histone deacetylase inhibitor ITF2357 in rheumatoid arthritis fibroblast-like synoviocytes: beyond transcriptional regulation. *Arthritis Res Ther* 20:148.
- Arcidiacono O, Krejčí J, Suchánková J, Bártová E (2018) Deacetylation of histone h4 accompanying cardiomyogenesis is weakened in HDAC1-depleted ES cells. *Int J Mol Med Sci* 19:E2425.
- Aune SE, Herr DJ, Kutz CJ, Menick DR (2015) Histone deacetylases exert class-specific roles in conditioning the brain and heart against acute ischemic injury. *Front Neurol* 6:145.
- Bederson JB, Pitts LH, Tsuji M, Nishimura MC, Davis RL, Bartkowski H (1986) Rat middle cerebral artery occlusion: evaluation of the model and development of a neurologic examination. *Stroke* 17:472-476.
- Bora KS, Sharma A (2011) Evaluation of antioxidant and cerebroprotective effect of *Medicago sativa* Linn. against ischemia and reperfusion insult. *Evid Based Complement Alternat Med* 2011:792167.
- Cheng YD, Al-Khoury L, Zivin JA (2004) Neuroprotection for ischemic stroke: two decades of success and failure. *NeuroRx* 1:36-45.
- Ding YH, Ding Y, Li J, Bessert DA, Rafols JA (2006) Exercise pre-conditioning strengthens brain microvascular integrity in a rat stroke model. *Neurol Res* 28:184-189.
- Evans MA, Broughton BR, Drummond GR, Ma H, Phan TG, Wallace EM, Lim R, Sobey CG (2018) Amnion epithelial cells - a novel therapy for ischemic stroke? *Neural Regen Res* 13:1346-1349.
- Grossman AW, Broderick JP (2013) Advances and challenges in treatment and prevention of ischemic stroke. *Ann Neurol* 74:363-372.
- Kassis H, Shehadah A, Li C, Zhang Y, Cui Y, Roberts C, Sadry N, Liu X, Chopp M, Zhang ZG (2016) Class IIA histone deacetylases affect neuronal remodeling and functional outcome after stroke. *Neurochem Int* 96:24-31.
- Kikuchi S, Suzuki R, Ohguchi H, Yoshida Y, Lu D, Cottini F, Jakubikova J, Bianchi G, Harada T, Gorgun G (2015) Class IIA HDAC inhibition enhances ER stress-mediated cell death in multiple myeloma. *J Leuk* 29:1918-1927.
- Kuang S, Wang Z, Su L, Han X, Dong Q (2018) Neuroprotection of histone deacetylase inhibitor TMP269 in cerebral ischemia/reperfusion rat. *Int J Clin Exp Med* 11:3405-3413.
- Lanzillotta A, Pignataro G, Branca C, Cuomo O, Sarnico I, Benarese M, Annunziato L, Spano P, Pizzi M (2013) Targeted acetylation of NF-kappaB/RelA and histones by epigenetic drugs reduces post-ischemic brain injury in mice with an extended therapeutic window. *Neurobiol Dis* 49:177-189.
- Lanzillotta A, Sarnico I, Ingrassia R, Boroni F, Branca C, Benarese M, Faraco G, Blasi F, Chiarugi A, Spano P (2010) The acetylation of RelA in Lys310 dictates the NF-kB-dependent response in post-ischemic injury. *Cell Death Dis* 1:e96.
- Liu L, Liu H, Yang F, Chen G, Zhou H, Tang M, Zhang R, Dong Q (2011) Tissue kallikrein protects cortical neurons against hypoxia/reoxygenation injury via the ERK1/2 pathway. *Biochem Biophys Res Commun* 407:283-287.
- Liu L, Zhang R, Liu K, Zhou H, Tang Y, Su J, Yu X, Yang X, Tang M, Dong Q (2009) Tissue kallikrein alleviates glutamate-induced neurotoxicity by activating ERK1. *J Neurosci Res* 87:3576-3590.
- Lobera M, Madauss KP, Pohlhaus DT, Wright QG, Trocha M, Schmidt DR, Baloglu E, Trump RP, Head MS, Hofmann GA (2013) Selective class IIA histone deacetylase inhibition via a nonchelating zinc-binding group. *Nat Chem Biol* 9:319-325.
- Mendis S, Davis S, Norrving B (2015) Organizational update: the world health organization global status report on noncommunicable diseases 2014; one more landmark step in the combat against stroke and vascular disease. *Stroke* 46:e121-122.
- Milan M, Pace V, Maiullari F, Chirivi M, Baci D, Maiullari S, Madaro L, Maccari S, Stati T, Marano G (2018) Givinostat reduces adverse cardiac remodeling through regulating fibroblasts activation. *Cell Death Dis* 9:108.
- Numagami Y, Ohnishi ST (2001) S-allylcysteine inhibits free radical production, lipid peroxidation and neuronal damage in rat brain ischemia. *J Nutrition* 131:1100S-1105S.
- Oh BR, Suh D-h, Bae D, Ha N, Choi YI, Yoo HJ, Park JK, Lee EY, Lee EB, Song YW (2017) Therapeutic effect of a novel histone deacetylase 6 inhibitor, CKD-L, on collagen-induced arthritis in vivo and regulatory T cells in rheumatoid arthritis in vitro. *Arthritis Res Ther* 19:154.
- Orillion A, Hashimoto A, Damayanti N, Shen L, Adelaiye-Ogala R, Arisa S, Chintala S, Ordentlich P, Kao C, Elzey B (2017) Entinostat neutralizes myeloid-derived suppressor cells and enhances the anti-tumor effect of PD-1 inhibition in murine models of lung and renal cell carcinoma. *Clin Cancer Res* 23:5187-5201.
- Pili R, Quinn DI, Hammers HJ, Monk P, George S, Dorff TB, Olencki T, Shen L, Orillion A, Lamonica D (2017) Immunomodulation by entinostat in renal cell carcinoma patients receiving high-dose interleukin 2: a multicenter, single-arm, phase I/II trial (NCI-CTEP# 7870). *Clin Cancer Res* 23:7199-7208.
- Rajendran P, Rengarajan T, Thangavel J, Nishigaki Y, Sakthisekaran D, Sethi G, Nishigaki I (2013) The vascular endothelium and human diseases. *Int J Biol Sci* 9:1057-1069.
- Rana DS, Anand I, Batra A, Sethi PK, Bhargava S (2018) Serum levels of high-sensitivity C-reactive protein in acute ischemic stroke and its subtypes: a prospective case-control study. *Asia Pac J Clin Trials Nerv Syst Dis* 3:128-135.
- Rawal S, Munasinghe PE, Nagesh PT, Lew JKS, Jones GT, Williams MJ, Davis P, Bunton D, Galvin IE, Manning P (2017) Down-regulation of miR-15a/b accelerates fibrotic remodelling in the Type 2 diabetic human and mouse heart. *Clin Sci* 131:847-863.
- Sando III R, Gounko N, Pieraut S, Liao L, Yates III J, Maximov A (2012) HDAC4 governs a transcriptional program essential for synaptic plasticity and memory. *Cell* 151:821-834.
- Sierra C, Coca A, Schiffrin EL (2011) Vascular mechanisms in the pathogenesis of stroke. *Curr Hypertens Rep* 13:200-207.
- Sinnett-Smith J, Ni Y, Wang J, Ming M, Young SH, Rozengurt E (2014) Protein kinase D1 mediates class IIA histone deacetylase phosphorylation and nuclear extrusion in intestinal epithelial cells: role in mitogenic signaling. *Am J Physiol Cell Physiol* 306:C961-C971.
- Smith WS (2004) Pathophysiology of focal cerebral ischemia: a therapeutic perspective. *J Vasc Interv Radiol* 15:S3-S12.
- Su J, Tang Y, Liu L, Zhou H, Dong Q (2011) Regulation of acid-sensing ion channel 1a function by tissue kallikrein may be through channel cleavage. *Neurosci Lett* 490:46-51.

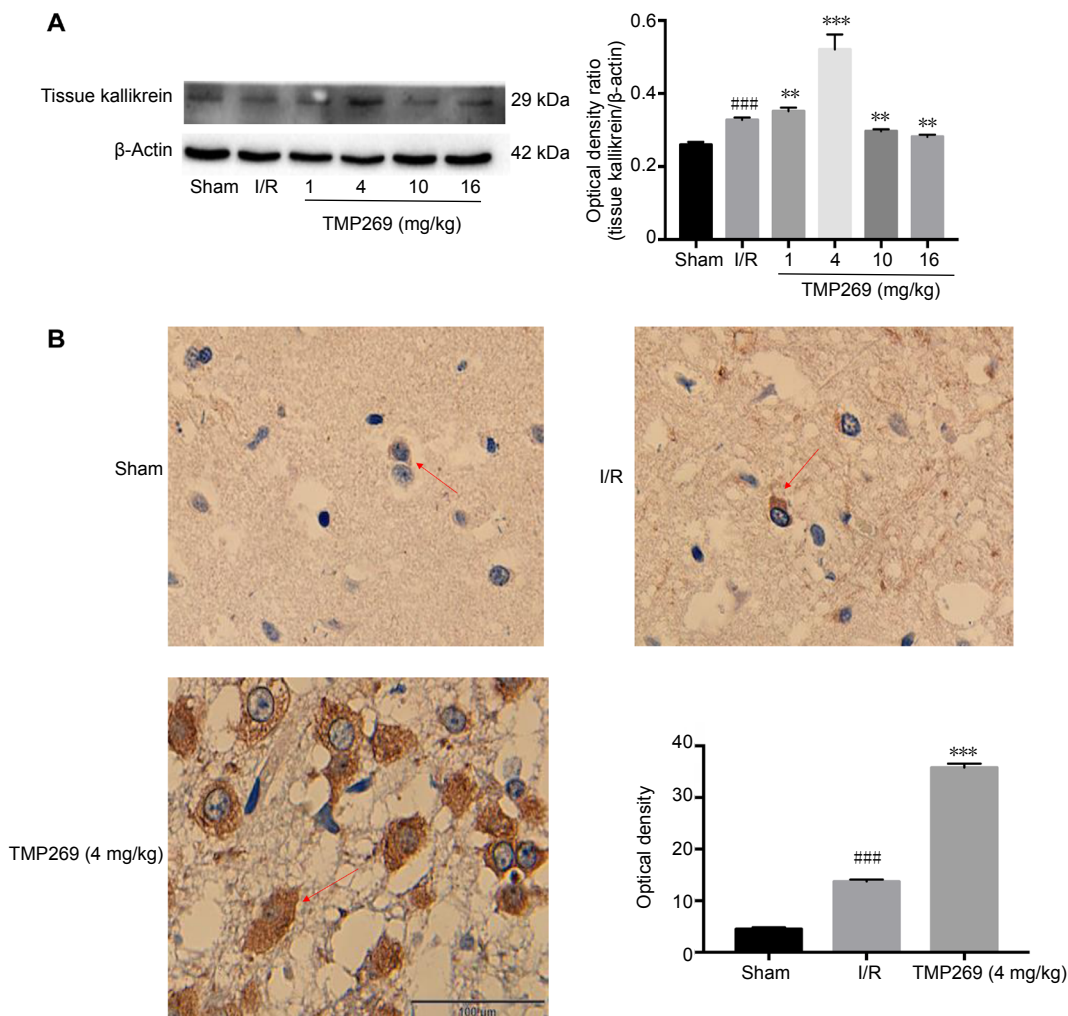


Figure 4 TMP269 up-regulates the expression of tissue kallikrein.

(A) Western blot analysis of tissue kallikrein. (B) Immunohistochemistry images and quantitative analysis of mean optical density. The number of positive cells in the infarct area increased and the plasma was deeply stained in the TMP269 group. The red arrows indicate cytoplasm; tissue kallikrein is expressed in cytoplasm; and the darker the color, the more expression of tissue kallikrein. Scale bar: 100 μ m. Data are expressed as the mean \pm SD. ** P < 0.01, *** P < 0.001, vs. ischemia/reperfusion (I/R) group; ### P < 0.001, vs. sham group.

Sugo N, Oshiro H, Takemura M, Kobayashi T, Kohno Y, Uesaka N, Song WJ, Yamamoto N (2010) Nucleocytoplasmic translocation of HDAC9 regulates gene expression and dendritic growth in developing cortical neurons. *Eur J Neurosci* 31:1521-1532.

Večeřa J, Bártová E, Krejčí J, Legartová S, Komůrková D, Rudá-Kučerová J, Štark T, Dražanová E, Kašpárek T, Šulcová A (2018) HDAC1 and HDAC3 underlie dynamic H3K9 acetylation during embryonic neurogenesis and in schizophrenia-like animals. *J Cell Physiol* 233:530-548.

Wang YZ, Zhang HY, Liu F, Li L, Deng SM, He ZY (2019) Association between PPARG genetic polymorphisms and ischemic stroke risk in a northern Chinese Han population: a case-control study. *Neural Regen Res* 14:1986-1993.

Yi F, Zhang AY, Janscha JL, Li P-L, Zou A-P (2004) Homocysteine activates NADH/NADPH oxidase through ceramide-stimulated Rac GTPase activity in rat mesangial cells. *Kidney Int* 66:1977-1987.

Zhang DL, Li D, Wang MJ (2018a) Mechanism and application of stem cell transplantation in the treatment of ischemic stroke. *Zhongguo Zuzhi Gongcheng Yanjiu* 22:5393-5398.

Zhang L, Zhang J, Jiang Q, Zhang L, Song W (2018b) Zinc binding groups for histone deacetylase inhibitors. *J Enzyme Inhib Med Chem* 33:714-721.

P-Reviewers: Mehan S, Ye M; C-Editor: Zhao M; S-Editors: Wang J, Li CH; L-Editors: Allen J, Maxwell R, Qiu Y, Song LP; T-Editor: Jia Y